Laser and Particle Beams (2016), *34*, 513–518.

doi:10.1017/S0263034616000379

Tail modulation suppression in the process of high-energy stimulated Brillouin scattering pulse compression

Z.H. LIU,[1] Y.L. WANG,[1] H.L. WANG,[1] H. YUAN,[1] R. LIU,[1] S.S. LI,[1] Z. BAI,[1] R.Q. FAN,[2] W.M. HE,[1] AND Z.W. LU[1]

[1]Technology on Tunable Laser, Harbin Institute of Technology, Harbin 150001, People's Republic of China
[2]Department of Chemistry, Harbin Institute of Technology, Harbin 150001, People's Republic of China

(Received 12 April 2016; Accepted 28 May 2016)

Abstract

We report that the tail modulation of Stokes pulses in the high-energy stimulated Brillouin scattering pulse compression can be suppressed by controlling effective pulse width of the pump. It is shown through numerical simulations and validated experimentally that the effective pulse width is an appropriate parameter, which determines the generation of tail modulation. The effective pulse width broaden as the increase of energy. This mechanism leads to the amplification of Stokes tail edge and it is the cause of tail modulation.

Keywords: Stimulated Brillouin scattering; Tail modulation suppression; Pulse compression

1. INTRODUCTION

During the past decades, many attentions have been drawn to developing sub-nanosecond laser pulse generation techniques for applications, including high harmonic generation with high spectral purity of atomic and molecular spectroscopy (Ganeev *et al*., 2014; Bertolotti, 2015) efficient pump source of parametric amplifier (Ishii *et al*., 2005; Popmintchev *et al*., 2012) and high spatial resolution in the LIDAR Thomson scattering diagnostics. Stimulated Brillouin scattering (SBS) pulse compression is particularly compelling in sub-nanosecond laser pulse generation because of its easy realization, low expenditure, high-energy load (Guillaume *et al*., 2014), and arbitrary wavelength operation (Gorbunov *et al*., 1983; Davydov *et al*., 1986; Roy *et al*., 1986; Yuan *et al*., 2014; Hasi *et al*., 2015). With the development of SBS pulse compression, the maximum Stokes pulse energy has been achieved from <1 mJ (Velchev *et al*., 1999) to more than 1 J (Feng *et al*., 2014) with the minimum compressed pulse width from several nanoseconds (Damzen & Hutchinson, 1983; Yoon *et al*., 2009) to hundreds picoseconds (Zhu *et al*., 2015). In these reports, however, laser pulses without tail modulation in the process of SBS pulse compressing are acquired only at low intensities (Schiemann *et al*., 1997).

With the increase of the pump energy, tail modulation of the Stokes pulse, which limits the output pulse power and width in the compressing as a result of the pump energy depletion and pulse width broadening, becomes more serious (Ottusch & Rockwell, 1991; Kuwahara *et al*., 2000; Mitra *et al*., 2006; Laroche *et al*., 2011) Dane *et al*. (1992) proposed a two-cell structure and presented that the wave profile trailing edge would broaden and lengthen with the increasing of the pump energy. Also, Yoshida *et al*. (2007) found that the Stokes pulse broadening at higher pump energy in the quartz was attributed to the Stokes trailing-edge amplification caused by the residual pump. The tail modulation phenomenon still existed in Yoshida's (2009) later study that the pump pulse with the energy of 1 J was compressed from 13 ns to 160 ps. Xu *et al*. (2014) also noticed the phenomenon in high-energy SBS compression and indicated that tail modulation could decrease when the Stokes pulse duration was shorter than the phonon lifetime. In those reports, tail modulation in high-energy SBS compression is due to insufficient amplification of the Stokes leading edge and high pump energy simply. However, the mechanism of tail modulation generation and its suppression scheme were seldom investigated in SBS.

In this paper, we present an analysis of tail modulation generation as well as a numerical model for the Stokes waveform. In our experiment, a double-stage compression

Address correspondence and reprint requests to: Y.L. Wang, National Key Laboratory of Science and Technology on Tunable Laser, Harbin Institute of Technology, P. O. Box 3031, Harbin 150080, People's Republic of China. E-mail: wyl@hit.edu.cn

structure is conducted in order to validate numerical results. The first stage is used to control effective pump width within a rational range, and the second stage can achieve a steep leading-edge pulse without tail modulation. For the first time to our knowledge, we have demonstrated pulse compression from 8 ns to 102 ps accompanying no tail modulation and achieved a 90% maximum reflectivity with effective energy reflectivity of 42%.

2. ANALYSIS AND SIMULATIONS

We define the effective pulse width of the pump to explain the Stokes tail modulation resulted from the SBS pulse compression. Effective pump width is defined as the part of the pump whose intensity reaches and exceeds the SBS threshold. It means that Stokes can be amplified by the pump immediately in the duration of the effective pump width once they encounter each other. The energy of the main peak range of the compressed pulse is concerned as the effective Stokes energy, and we define the ratio of the energy to the incident energy as effective energy reflectivity whose value shows the degree of Stokes tail modulation and characterizes the energy transform after SBS compression accurately. Figure 1 is the schematic diagram of effective pulse width of the pump changing with the energy. The generation time of Stokes pulse depends on the pump power injecting into the cell. If the pump power exceeds the threshold at the peak point "*f*", the generation time equals the distance between point "*f*" and the focal point "*a*". In this condition, the effective pulse width of the pump is close to zero and the Stokes leading edge cannot be amplified. So the emitted Stokes exhibits almost the same waveform as the pump light. With increasing of the pump energy (power), the time exceeding SBS threshold moves forward from point "*f*" to point "*b*" and the effective pump width (Δt) is $\Delta t1$, $\Delta t2$, $\Delta t3$, $\Delta t4$ accordingly. Under these conditions, backscattering stokes pulse leading edge is amplified and the corresponding pulse width is narrowed. When the effective pulse width of pump is equal to the back-turning time in cell, Stokes pulse is compressed sufficiently. The pump energy increases further and the Stokes leading-edge has transmitted the cell before the pump enters the cell completely. The Stokes trailing edge is amplified by the residual pump, which results in the tail modulation. In the case of Gaussian pump, effective pulse width of the pump continues to grow with the pump intensity, as shown in Figure 2.

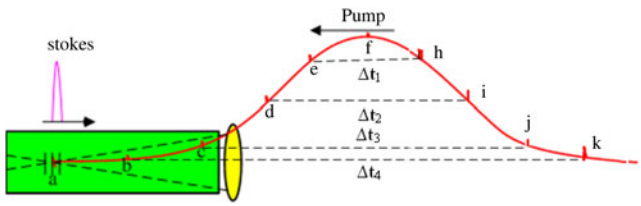

Fig. 1. Effective pulse width of the pump at different energy.

Therefore, the key of suppression of the tail modulation generation is to let the pump effective pulse width in a proper range. Pulse temporal compression of the pump can decrease its effective pulse width bellow the back-turning time. It is convenient to use a stage SBS compression with long focal distance lens to shorten the pump's effective pulse width and retain most of energy. It should be noted that the compression degree of the Gaussian pump has an important impact on the output result. Here, we studied two general and typical situations. When the leading edge of Gaussian pump light is cut partly, this condition is called unilateral semi-cut Gaussian pump. If the leading edge of Gaussian pump light is cut completely, this condition is called unilateral full-cut pump. In the experiment, the compression degree of Gaussian pump can be controlled by the focal length of lens. Because of the limited interaction

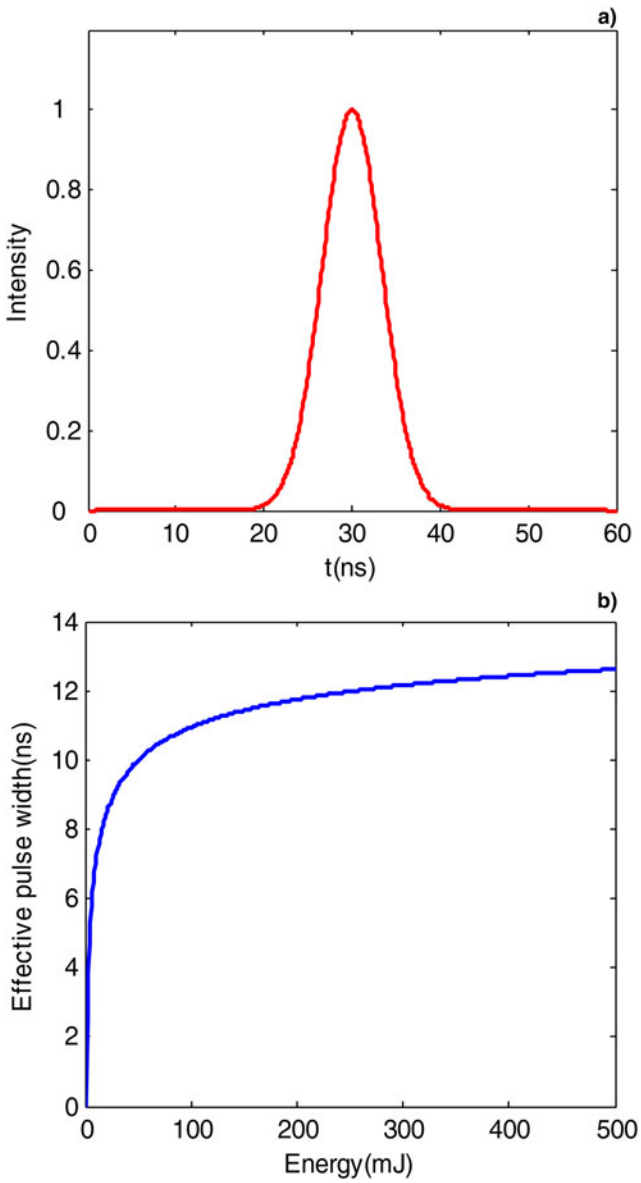

Fig. 2. (a) Gaussian pump. (b) The effective pulse width of Gaussian pump.

https://doi.org/10.1017/S0263034616000379 Published online by Cambridge University Press

length, short focal length lens cut the leading edge of Gaussian pump partly and long focal length lens can do it completely.

To validate our analysis, we simulate the process of SBS compression by classical model (Ottusch & Rockwell, 1991). The SBS process involves counter-propagating two optical fields E_L (laser) and E_S (Stokes), which are coupled through the electrostriction with an acoustic field $\overline{\rho}$.

$$E_L(z,t) = E_L(z,t)e^{i(k_L z-\omega_L t)} + c.c., \tag{1a}$$

$$E_S(z,t) = E_S(z,t)e^{i(-k_S z-\omega_S t)} + c.c., \tag{1b}$$

$$\overline{\rho}(z,t) = \rho_0 + \rho(z,t)e^{i(q_B z-\Omega_B t)} + c.c. \tag{1c}$$

Optical field E_L and E_S are governed by Maxwell's equations, and acoustic field $\overline{\rho}$ obeys the Navier–Stokes equation. Wave equations can be written in the form as Eq. (2).We solved Eq. (2) numerically by a generalization of the split-step method.

$$\frac{\partial E_L}{\partial z} + \frac{\alpha}{2}E_L + \left(\frac{n}{c}\right)\frac{\partial E_L}{\partial t} = \frac{i\omega_L\gamma^e}{2nc\rho_0}\rho E_S, \tag{2a}$$

$$-\frac{\partial E_S}{\partial z} + \frac{\alpha}{2}E_S + \left(\frac{n}{c}\right)\frac{\partial E_S}{\partial t} = \frac{i\omega_S\gamma^e}{2nc\rho_0}\rho^* E_L, \tag{2b}$$

$$\frac{\partial^2\rho}{\partial t^2} - (2i\omega - \Gamma_B)\frac{\partial\rho}{\partial t} - (i\omega\Gamma_B)\rho = \frac{\gamma^e}{4\pi}q_B^2 E_L E_S^*. \tag{2c}$$

We numerically simulate the Stokes waveform, pulse width, energy reflectivity, and effective energy reflectivity of Gaussian pump, unilateral semi-cut Gaussian pump and unilateral full-cut pump, respectively. FC-72 is chosen as the active medium. The length of cell and the focal length of the lens are 100 and 60 cm in the simulation, respectively. Parameters of FC-72 are in Table 1.

Figure 3 shows the dependences of curve waveform of Gaussian pump, unilateral semi-cut pump, unilateral full-cut pump on the Stokes pulse width, energy reflectivity, effective energy reflectivity, and the pump peak power. As shown in

Table 1. *Physical properties of FC-72*

Fluorinert property	FC-72
Absorption coefficient (cm^{-1})	$<10^{-3}$
OBT (GW/cm^2)	>100
Threshold energy (10 ns, mJ)	2.5
Brillouin shift (MHz)	1100
SBS gain Coefficient (cm/GW)	6
Brillouin Linewidth (MHz)	270
Phonon lifetime (ns)	1.2

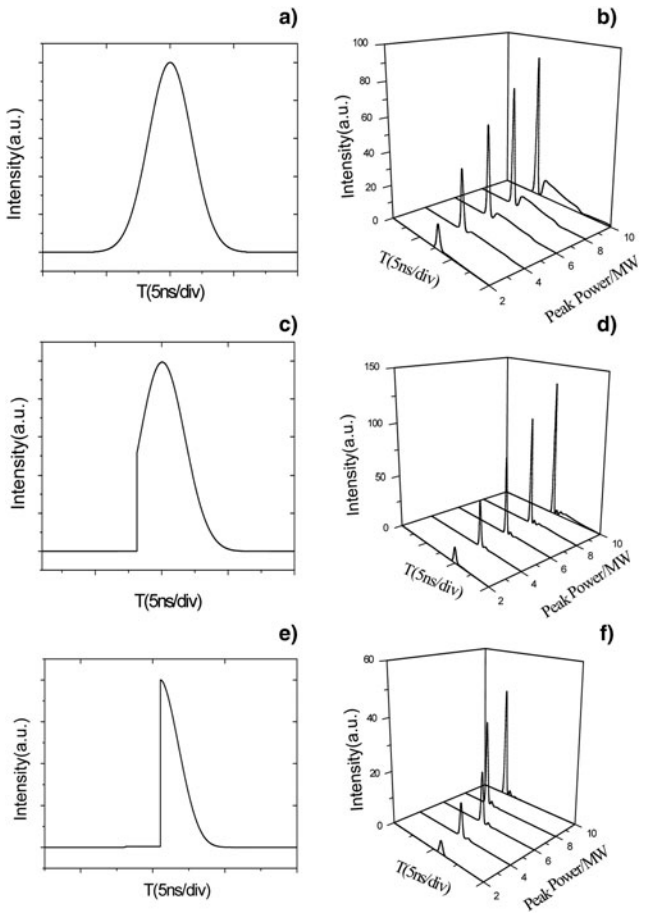

Fig. 3. The wave form of (a, b) Gaussian pump and corresponding Stokes pulse. (c, d) Unilateral semi-cut pump Gaussian pump and corresponding Stokes pulse. (e, f) Unilateral full-cut pump Gaussian pump and corresponding Stokes pulse.

Figure 3b, with the increasing of the pump peak power, there is a tail modulation in the Stokes profile obviously when higher Gaussian pump is injected. Unilateral semi-cut pump and the corresponding Stokes pulse depending on pump peak power are shown in Figure 3c, 3d separately. Compared with Figure 3b, the Stokes tail modulation is suppressed significantly and the main peak is amplified evidently, which leads to narrower pulse width and higher peak power. The peak power and the Stokes waveform with the injection of unilateral full-cut pump demonstrate (Fig. 3e, 3f) that, compared with Gaussian pump, unilateral full-cut pump method can suppress the tail modulation but without amplifying the output Stokes pulse sufficiently caused by the excessive pump reduction.

3. EXPERIMENTAL SETUP AND RESULTS

The schematic layout is shown in Figure 4. A Q-switched, injection-seeded Nd: YAG laser (Continuum PRII9010) at 1064 nm is operated in a single longitudinal mode; its pulse duration is 8 ns with repetition of 1 Hz. The cell is filled with fluorinated liquid (FC-72) medium with a short

https://doi.org/10.1017/S0263034616000379 Published online by Cambridge University Press

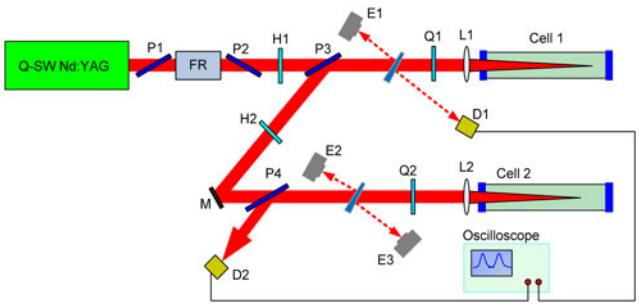

Fig. 4. Experimental setup of double compressor; P, polarizing beam splitter; L, convex lens; H, half wave-plate; Q, quarter-wave plate; E, energy meter; Cell, Brillouin compressor; D, photo detector.

phonon lifetime (1.2 ns). The combination of a Faraday rotator FR and a polarizer P1 as an isolator avoids the backscattered radiation back to the laser resonator. A polarizer P3 and a half wave plate are used together to adjust the pump energy. The circularly polarized laser beam is focused into the cell1 using a lens L1 (focal length = 300 and 600 mm). Reflected by the polarizer P3 and a mirror M, the output Stokes light is injected into the second cell (1 m) by the L2, 60 cm convex lens. The final Stokes is extracted by a polarizer P4.

In experiment, we use Israel Ophir energy detector ED500 (E1, E2, and E3) to monitor the pump energy, the first-stage compression and the Stokes in the second-stage compression, respectively. Stokes pulse shapes both in the first and the second stage are monitored using two PIN photodiodes and a digital phosphor oscilloscope TDS3032B. The effective energy reflectivity can be obtained through the area ratio of the main peak to entire waveform.

4. DISCUSSION

In the experiment, waveforms of unilateral semi-cut Gaussian pump and unilateral full-cut Gaussian pump can be achieved when the focal length of L1 is 300 and 600 mm, respectively. When pump energy is 300 mJ, the reshaped pump waveform and corresponding Stokes pulses are shown in Figure 5. One can see from Figure 5a, 5b that there is serious tail modulation in a temporal trace of the Stokes pumped by Gaussian pump, which is in reasonable agreement with the result of simulations shown in Figure 3b. But in Figure 5c, 5d, the experimental Stokes waveform pumped by unilateral semi-cut pump pulse demonstrates high peak value, narrow pulse width, and no tailing modulation. In Figure 5e, 5f, it is coincides with the expectation that the Stokes temporal trace of unilateral full-cut pump injection creates no tailing modulation. The output pulse width pumped by Gaussian pump, unilateral semi-cut Gaussian pump, and unilateral full-cut Gaussian pump are 257, 102, and 198 ps, respectively. This manifests that the reduction in the effective pump width results in a significant suppression of the Stokes tail modulation, which makes it possible to achieve shorter Stokes pulse. It should be noted that when effective pump

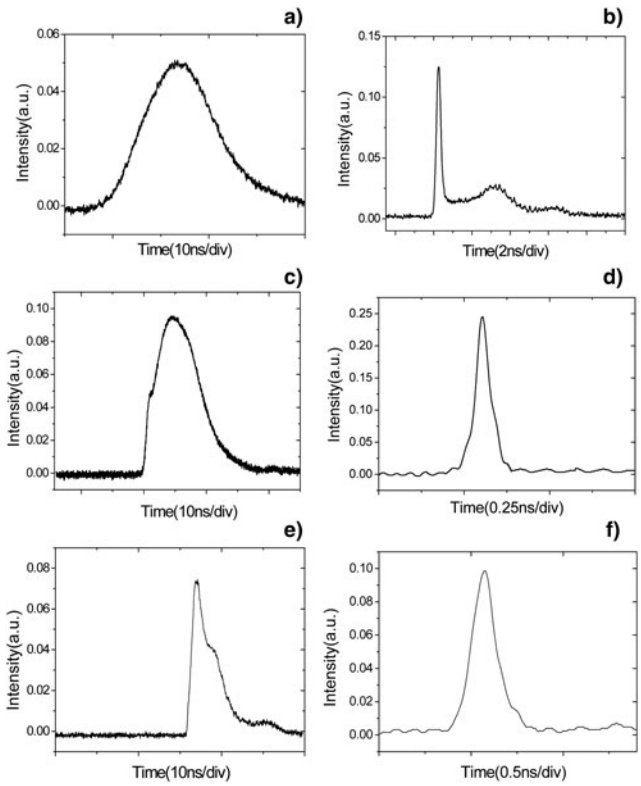

Fig. 5. Oscillograms of the pump pulses (on the left) and corresponding Stokes pulses (on the right) (a) Gaussian pump and corresponding Stokes (257 ps). (b) Unilateral semi-cut Gaussian pump and compressed Stokes (102 ps) and (c) unilateral full-cut Gaussian pump and corresponding Stokes (198 ps).

pules width is controlled in a rational range, excessive cut of pump is unfavorable to the further compression instead.

Figure 6 shows that the Stokes width of unilateral cut pump gets a more significant compression and is only a half of it compressed from Gaussian pump in the same

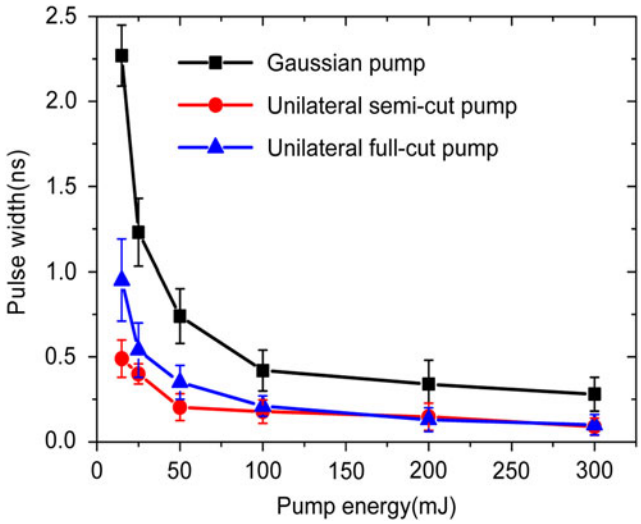

Fig. 6. Dependences of the Stokes pulse width on incident pump energy.

https://doi.org/10.1017/S0263034616000379 Published online by Cambridge University Press

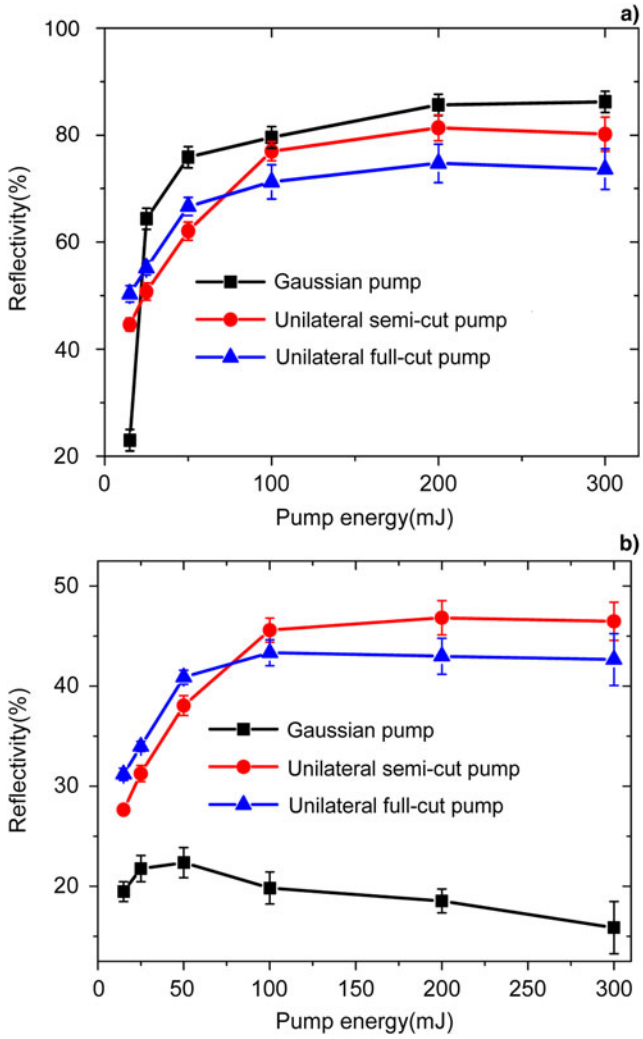

Fig. 7. Dependences of (a) energy reflectivity and (b) effective energy reflectivity on incident pump energy.

condition. This is related to their sloping leading-edge, which causes more rapid establishment of acoustic field and faster generation of Stokes pulse.

Effective energy reflectivity is an appropriate parameter to analyze modulation degree quantitatively. Figure 6 presents the experimental measurement of effective energy reflectivity and Stokes pulse width pumped by different pump waveforms. While the Gaussian pump energy reflectivity could increase as the increasing of pump energy until reaching 90% in 300 mJ in Figure 7a, the corresponding effective energy reflectance, as shown in Figure 7b, merely emerges a slow escalating trend until the pump energy reaches 50 mJ, and then sustains to decline with the pump energy increasing. Consecutive drop of effective energy reflectivity in high-energy indicates an increasingly serious tailing modulation. In the case of Gaussian pump, the effective pulse width of pump continues to grow with the pump energy, as shown in Figure 2b, and the unwanted amplification of Stokes tailing edge becomes inevitable. By contrast, the effective energy reflectivity of unilateral cut pump manifests an exponential rising trend and can reach a high value (nearly 50% in pump energy of 300 mJ).

In the process of unilateral cut pump, the Gaussian pump is converted during the first-stage compression into a short pulse. The effective pulse width of unilateral cut pump can remain at a proper value and is not sensitive to the increase of the pump energy any more. So the effective pulse width of pump is not long enough to amplify the Stokes tailing edge even at high pump energy, and the tailing modulation can be suppressed. It can be said that if the effective pump duration is in a rational range, unilateral cut pump is more favorable to achieve highly effective energy conversion efficiency due to better amplification and longer interaction length of Stokes and pump.

5. CONCLUSION

In conclusion, we have investigated a method using the effective pump width control to suppress the tail modulation in the process of high-energy SBS pulse compression. It has been demonstrated that the effective pump width control can be achieved by one compressor. It has been shown that when effective pump width is controlled in a rational range, the tail modulation can be suppressed well. Moreover, appropriate control of effective pump width is conducive to achieve high compression radio and effective energy reflectivity.

ACKNOWLEDGMENTS

This work was supported by the National Natural Science Foundation of China (Grants No. 61378007, 61378016, and 61138005), the Fundamental Research Funds for the Central Universities (Grant No. HIT. IBRSEM. A. 201409).

REFERENCES

Bertolotti, M. (2015). High-order harmonic generation in laser plasma plumes, by Rashid Ganeev: Scope: Review. Level: Early career researcher, researcher, teacher, specialist. *Contemp. Phys*. **56**, 88–89.

Damzen, M.J. & Hutchinson, M.H.R. (1983). High-efficiency laser-pulse compression by stimulated Brillouin scattering. *Opt. Lett*. **8**, 313–315.

Dane, C.B., Neuman, W.A., Hackel, L.A., Norton, M.A. & Miller, J.L. (1992). Energy scaling of SBS pulse compression. *Proc. SPIE* **1626**. 297–307.

Davydov, M.A., Shipilov, K.F. & Shmaonov, T.A. (1986). Formation of highly compressed stimulated Brillouin scattering pulses in liquids. *Sou. J. Quantum Electron*. **16**, 1402–1403.

Feng, C., Xu, X. & Diels, J.C. (2014). Generation of 300 ps laser pulse with 1.2 J energy by stimulated Brillouin scattering in water at 532 nm. *Opt. Lett*. **39**, 3367–3370.

Ganeev, R.A., Suzuki, M. & Kuroda, H. (2014). Advanced properties of extended plasmas for efficient high-order harmonic generation. *Phys. Plasmas* **21**, 053503.

Gorbunov, V.A., Papernyĭ, S.B., Petrov, V.F. & Startsev, V.R. (1983). Time compression of pulses in the course of stimulated

https://doi.org/10.1017/S0263034616000379 Published online by Cambridge University Press

Brillouin scattering in gases. *Sou. J. Quantum Electron*. **13**, 900–905.

Guillaume, E., Humphrey, K., Nakamura, H., Trines, R.M.G.M., Heathcote, R., Galimberti, M. & Kar, S. (2014). Demonstration of laser pulse amplification by stimulated Brillouin scattering. *High Power Laser Sci. Eng*. **2**, e33.

Hasi, W., Zhao, H., Lin, D., He, W. & Lü, Z. (2015). Characteristics of perfluorinated amine media for stimulated Brillouin scattering in hundreds of picoseconds pulse compression at 532 nm. *Chin. Opt. Lett*. **13**, 061901–061901.

Ishii, N., Turi, L., Yakovlev, V.S., Fuji, T., Krausz, F., Baltuška, A. & Piskarskas, A. (2005). Multimillijoule chirped parametric amplification of few-cycle pulses. *Opt. Lett*. **30**, 567–569.

Kuwahara, K., Takahashi, E., Matsumoto, Y., Kato, S. & Owadano, Y. (2000). Short-pulse generation by saturated KrF laser amplification of a steep Stokes pulse produced by two-step stimulated Brillouin scattering. *JOSA B* **17**, 1943–1947.

Laroche, M., Gilles, H. & Girard, S. (2011). High-peak-power nanosecond pulse generation by stimulated Brillouin scattering pulse compression in a seeded Yb-doped fiber amplifier. *Opt. Lett*. **36**, 241–243.

Mitra, A., Yoshida, H., Fujita, H. & Nakatsuka, M. (2006). Sub nanosecond pulse generation by stimulated Brillouin scattering using FC-75 in an integrated with laser energy up to 1.5 J. *Jpn. J. Appl. Phys*. **45**, 1607–1611.

Ottusch, J.J. & Rockwell, D.A. (1991). Stimulated Brillouin scattering phase-conjugation fidelity fluctuations. *Opt. Lett*. **16**, 369–371.

Popmintchev, T., Chen, M.C., Popmintchev, D., Arpin, P., Brown, S., Ališauskas, S. & Baltuška, A. (2012). Bright coherent ultrahigh harmonics in the keV x-ray regime from mid-infrared femtosecond lasers. *Science* **336**, 1287–1291.

Roy, D.G. & Rao, D.V.G.L.N. (1986). Optical pulse narrowing by backward, transient stimulated Brillouin scattering. *J Appl. Phys*. **59**, 332–335.

Schiemann, S., Ubachs, W. & Hogervorst, W. (1997). Efficient temporal compression of coherent nanosecond pulses in a compact SBS generator–amplifier setup. *IEEE J. Quantum Electron*. **33**, 358–366.

Velchev, I., Neshev, D., Hogervorst, W. & Ubachs, W. (1999). Pulse compression to the subphonon lifetime region by half-cycle gain in transient stimulated Brillouin scattering. *IEEE J. Quantum Electron*. **35**, 1812–1816.

Xu, X., Feng, C. & Diels, J.C. (2014). Optimizing sub-ns pulse compression for high energy application. *Opt. Express* **22**, 13904–13915.

Yoon, J.W., Shin, J.S., Kong, H.J. & Lee, J. (2009). Investigation of the relationship between the prepulse energy and the delay time in the waveform preservation of a stimulated Brillouin scattering wave by prepulse injection. *JOSA B* **26**, 2167–2170.

Yoshida, H., Fujita, H., Nakatsuka, M., Ueda, T. & Fujinoki, (2007). Compact temporal-pulse-compressor used in fused-silica glass at 1064 nm wavelength. *J. Appl. Phys*. **46**, L80–L82.

Yoshida, H., Hatae, T., Fujita, H., Nakatsuka, M. & Kitamura, S. (2009). A high-energy 160-ps pulse generation by stimulated Brillouin scattering from heavy fluorocarbon liquid at 1064 nm wavelength. *Opt. Express* **17**, 13654–13662.

Yuan, H., Lu, Z.W., Wang, Y.L., Zheng, Z.X. & Chen, Y. (2014). Hundred picoseconds laser pulse amplification based on scalable two-cells Brillouin amplifier. *Laser Part. Beams* **32**, 369–374.

Zhu, X., Lu, Z. & Wang, Y. (2015). High stability, single frequency, 300 mJ, 130 ps laser pulse generation based on stimulated Brillouin scattering pulse compression. *Laser Part. Beams* **33**, 11–15.

https://doi.org/10.1017/S0263034616000379 Published online by Cambridge University Press